

Megahertz electron modulations during TSS 1R

M. P. Gough,¹ W. J. Burke,² D. A. Hardy,² C. Y. Huang,³ L. C. Gentile,³
A. G. Rubin,² M. R. Oberhardt,⁴ A. T. Drobot,⁵ D. C. Thompson,⁶ and
W. J. Raitt⁶

Abstract. Experiments were conducted during the Tethered Satellite System Reflight in which a 1 keV, 100 mA electron beam was emitted from the shuttle at pitch angles near 90°. Rapid plasma responses measured by the Shuttle Potential and Return Electron Experiment (SPREE) show time-modulated electron fluxes within the beam flux tube. Megahertz modulations fall into two classes: (1) narrow-bands close to harmonics of the electron gyrofrequency f_{ce} and (2) broad-bands at interharmonic frequencies in which electrons of different energies had different modulation frequencies. When SPREE intercepted beam electrons after a single gyroturn they, too, were modulated at similar frequencies. Data suggest that beam electrons were modulated by strong plasma interactions near the emission aperture, generating time-varying electric fields that modulated other electrons near the beam cylinder. This is analogous to the electron cyclotron maser responsible for auroral kilometric radiation.

Introduction

Measurements by the Shuttle Potential and Return Electron Experiment (SPREE) during the first flight of the Tethered Satellite System (TSS 1) show that electron beams ejected from the shuttle create a broad range of energy/angle spectra of returning electrons [Hardy *et al.*, 1995]. When ejected at pitch angles α_B near 90° some of the beam electrons reach SPREE after a single gyroturn. To reach SPREE they had to be scattered by a virtual cathode in the immediate vicinity of the fast pulsed electron gun (FPEG) aperture. Under these $\alpha_B \approx 90^\circ$ conditions, some electrons reaching

SPREE were modulated at frequencies between 2 and 4 MHz [Gough *et al.*, 1995]. Beam-induced wave activity has also been detected at similar frequencies at locations remote from the shuttle. During the Spacelab 2 mission when the plasma diagnostic package (PDP) flew close to the guiding center field lines of beam electrons it detected broad spectra of whistlers propagating near the resonance cone and emissions in the upper-hybrid frequency band [Farrell *et al.*, 1988]. Whistler waves were also detected near electron beams emitted during ECHO rocket experiments [Goerke *et al.*, 1990].

TSS reflight (TSS 1R) experiments were designed to diagnose beam interactions with the environment during extended FPEG emissions at $\alpha_B \approx 90^\circ$. We present two cases of electron modulations at megahertz frequencies. The first occurred with the shuttle in darkness at southern midlatitudes. The magnetic field was aligned with the shuttle's long axis [cf. Figure 2 of Gough *et al.*, 1995]. The second data set was acquired as the shuttle crossed the equator near dawn. The magnetic field had components along the shuttle's long axis and into the payload bay [cf. Figure 6 of Gough *et al.*, 1995].

Instrumentation

The SPREE consists of two nested, triquadrangular, electrostatic analyzers (ESAs) that simultaneously measured fluxes of electrons and ions with energies between 10 eV and 10 keV over a $100^\circ \times 8.5^\circ$ angular fan. In the reported intervals, spectra were compiled at a rate of 1 s^{-1} in 32 logarithmically spaced energy channels. The 100° dimension of the angular fan was divided into 10 zones. ESAs A and B were mounted back to back on rotary tables that turned 6° s^{-1} with a constant phase angle of 180° so that spectra were sampled over $2\pi \text{ sr}$ in 30 s [Hardy *et al.*, 1995].

In parallel with normal counting, SPREE processes data to calculate autocorrelation functions (ACFs) at megahertz frequencies. These are determined by six separate processing elements on three electron detection streams from the ESAs. Times between electron arrivals are measured in units of counts of a clock running at twice the maximum frequency to be studied. Using a buncher technique, histograms of time separations between electron detections were accumulated for each of the 32 energy levels sampled by the ESAs. These histograms are equivalent to the summation of many one-bit ACFs. The correlator units cycled between frequencies 0 – 5 MHz and 0 – 10 MHz using the

¹Space Science Centre, University of Sussex, Brighton, UK.

²Phillips Laboratory, Hanscom AFB, Massachusetts.

³Boston College Institute for Scientific Research, Chestnut Hill, Massachusetts.

⁴Amptek, Inc., Bedford, Massachusetts.

⁵Science Applications International Corporation, McLean, Virginia.

⁶Center for Atmospheric and Space Sciences, Utah State University, Logan, Utah.

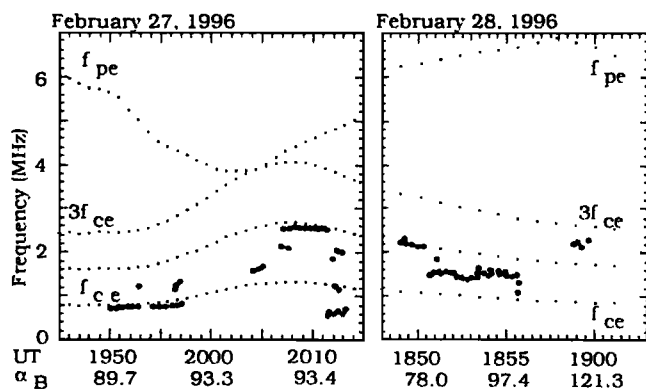


Figure 1. Observed electron modulation frequencies as functions of time and beam pitch angle for events 1 (left) and 2 (right). Superposed are harmonics of f_{ce} and f_{pe} .

counting cycles of 10 MHz and 20 MHz clocks. With SPREE measuring 1 electron energy spectrum s^{-1} , 3 s were needed to accumulate a modulation spectrum. Computer generated fast Fourier transform (FFT) processing of the 64-point histograms yields a 32-point frequency spectrum for each of the 32 energies for each accumulation period. The FFT resolution is thus $1/32$ of the maximum frequency: 312 (156) kHz in the 10 (5) MHz frequency range.

Observations

Frequencies of electron modulations were calculated manually by counting the lags (one lag unit is equivalent to a clock oscillation period) for several cycles across the ACF. Modulation frequencies for both events are plotted as functions of UT and α_B in Figure 1. Superposed lines indicate electron plasma frequency f_{pe} and harmonics of the electron cyclotron frequency f_{ce} . Values of f_{ce} and f_{pe} were calculated from magnetic field measurements by an onboard magnetometer, and plasma densities were estimated using the International Reference Ionosphere (IRI) model. Figure 1 shows that in the first event f_{ce} increased from 0.81 to 1.35 MHz. Plasma density decreased from $\sim 3 \times 10^5 \text{ cm}^{-3}$ at 1949 UT to $2 \times 10^5 \text{ cm}^{-3}$ at 2002 UT, then recovered. During the second event f_{ce} fell from 1.15 to 0.85 MHz while estimated density rose from 4.7 to $5.7 \times 10^5 \text{ cm}^{-3}$.

Before examining the events, we comment briefly on the frequencies plotted in Figure 1. First, there are extended intervals when a single frequency was detected below f_{ce} and either near or between harmonics of f_{ce} . Second, during a few intervals modulations occurred at several frequencies. Third, all modulations are well below estimates of f_{pe} .

Event 1: Day 58/1949 – 2011 UT

FPEG turned on at 1948:48 UT emitting a 100 mA beam of electrons at 1 keV for 14 steps, each with the

beam on for 26 s on and off for 14 s. After a several-minute hiatus, the sequence was repeated beginning at 2002:51 UT. During the second sequence the shuttle was in total darkness. Images from a low-light television camera show that FPEG emissions produced a streak of light almost parallel to the left side of the payload bay. This indicates that a large fraction of the beam electrons propagated in a cylindrical shell and impacted shuttle surfaces after almost a single gyrotorn. Data in Figure 1 show that during the first sequence most of the modulated fluxes of electrons returning to the shuttle were at frequencies near f_{ce} . In the second sequence the modulated fluxes were at frequencies near $2f_{ce}$, between f_{ce} and $2f_{ce}$, and below f_{ce} . Three ACFs taken between 2009:18 and 2010:14 UT are shown in Figure 2. The modulations at f_{ce} (middle) are precisely matched to alternate peaks of the modulations at $2f_{ce}$ (top). Modulation peaks $< f_{ce}$ (bottom) are not as closely matched and are at $0.43 f_{ce}$. Within any zone, all of the modulated electron fluxes were usually at the same frequency. However, there is some frequency mixing as shown in the middle plot of Figure 2. Weak modulations at $2f_{ce}$ can also be seen.

During event 1 modulation signals were detected at energies from several tens to a few hundred eV and near the beam energy. Of special interest are times

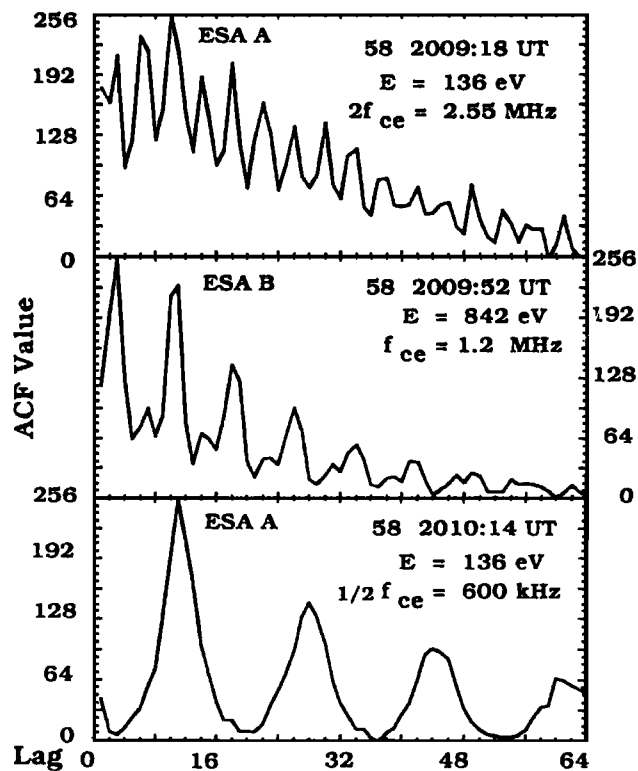


Figure 2. Examples of ACFs from event 1 showing strong modulations at frequencies related to f_{ce} harmonics for different electron energy-angles. The ACF operated in the 0 – 5 MHz range.

when ESA B (ESA A) looked toward the shuttle's left (right wing) and the magnetic field caused beam electrons to reach SPREE in the first gyrotorn [*Hardy et al.*, 1995]. When the flux of electrons with beam energy was $\geq 8 \times 10^9$ (cm² s sr eV)⁻¹, modulations were detected at 1.25 MHz during the first sequence and at 2.5 MHz during the second. At these times only one channel of ESA A detected modulated electron fluxes near 90 eV. Figure 3 plots ACFs measured simultaneously by ESA B at beam energy and by ESA A at 86 eV. When the beam intersected ESA A, the modulation frequencies were the same as those measured nearest in time by ESA B. Electron modulations at intermediate energies were detected by ESA A when it looked between the shuttle's left wing and the forward direction. Modulated fluxes were not detected when ESA A looked along the magnetic field [*Gough et al.*, 1995].

Event 2: Day 59/1849 – 1900 UT

In the second event FPEG operated in a 419 ms on/off cycle except for two intervals (1855:19 – 1858:53 UT and 1859:16 – 1859:36 UT) when it was off. Figure 1 shows that prior to 1850 and after 1858 UT the modulations were >2 MHz. From 1848 to 1850 UT the modulations closely followed $2f_{ce}$. After an abrupt transition, they were at frequencies in the 1.2 – 1.7 MHz range, between f_{ce} and $2f_{ce}$. These interharmonic modulations appeared when α_B was within 12° of perpendicular to the magnetic field. The characteristics of the modulations near $2f_{ce}$ are different from those between cyclotron harmonics. The bottom plot of Figure 4 shows that modulations at $2f_{pe}$ are dispersionless; ACFs show no phase differences between electrons with energies of 108 and 28 eV. Modulations at frequencies between the cyclotron harmonics show a discernible dis-

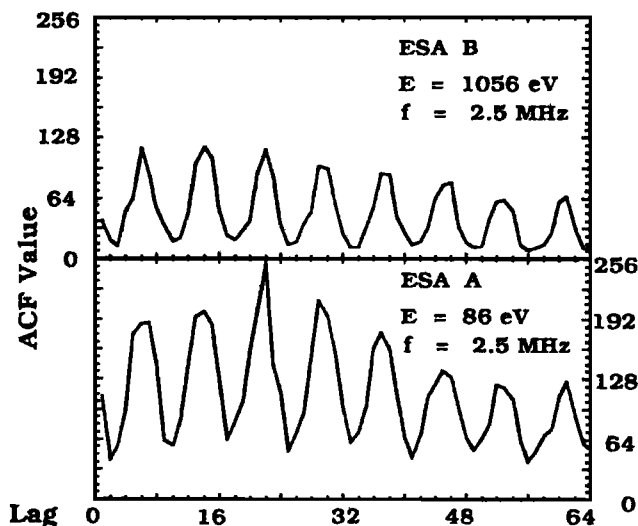


Figure 3. Examples of ACFs from event 1 at 2007:46 UT showing oscillations at $\sim 2 f_{ce}$ simultaneously measured by ESA B (top) at beam energy and by ESA A in zone 7 at 86 eV (bottom).

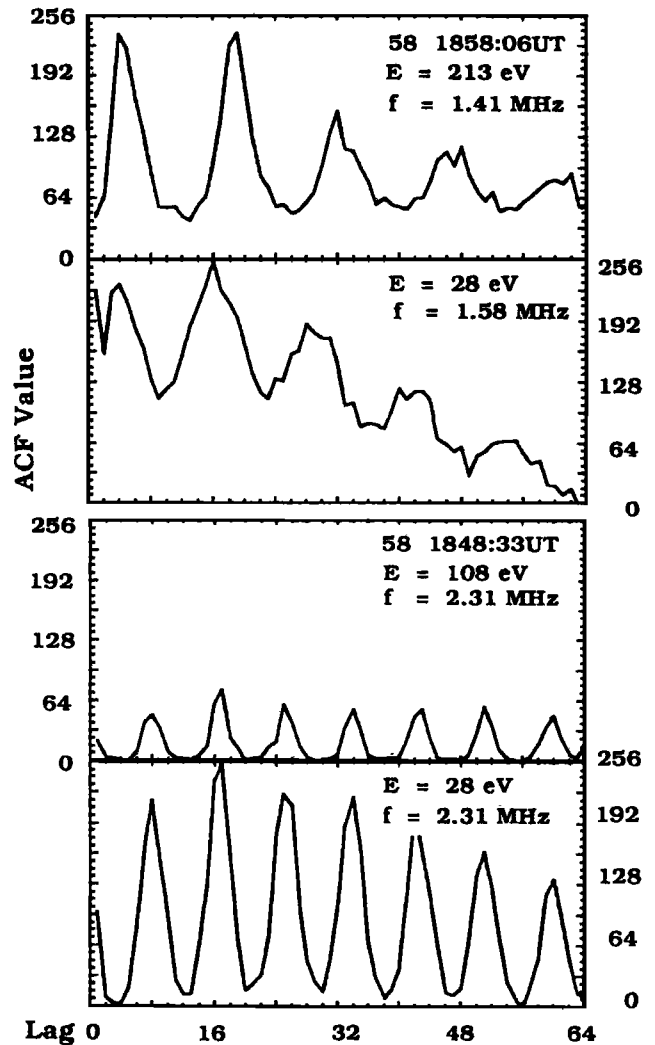


Figure 4. Examples of ACFs from event 2 showing that oscillations at $2 f_{ce}$ (bottom) are not dispersed while those at interharmonic frequencies (top) are.

persion, changing in frequency from 1.58 MHz at 28 eV to 1.41 MHz at 213 eV. The dispersion is not an artifact of pitch angle variation since α_B was stationary during the 12 s data accumulation. Nor is it the result of Doppler shifting from a frequency f^* due to the $v_{||}$ of the incoming electrons. Solving the Doppler-shift equations we find that the original wave would have to be a whistler propagating away from the shuttle with $f^* = 0.166$ MHz. We conclude that the ACF dispersion reflects causal oscillations that have a finite bandwidth of ~ 0.2 MHz. Both types in Figure 4 correspond to high levels of electron modulation, varying between 91% at 213 eV and 59% at 28 eV for cyclotron bands, while all were $>90\%$ at $\sim 2 f_{ce}$.

The magnetic field geometry allowed beam electrons to reach ESA B at flux levels sufficient to detect modulations from 1853 to 1855 UT. At these times ESA B looked just aft of the shuttle's left wing. Beam electrons were modulated at ~ 1.5 MHz and did not reach the aperture of ESA A. Modulations were simultane-

ously measured at the same frequency by ESA A at ~ 90 eV while looking toward the right wing.

Summary and Discussion

Although FPEG emissions were at smaller pitch angles during Spacelab 2, it is useful to consider PDP observations of whistler waves during conjunctions with the shuttle. *Farrell et al.* [1988] showed that electromagnetic power in the whistler band required a coherent Cerenkov emission process. That is, the whistler-emitting beam electrons must have been bunched by an intermediate electrostatic process. An analogous process for coherent whistler emissions from auroral electron beams [Maggs, 1976] required a much longer growth time than was available for FPEG electrons to transit the shuttle – PDP separation. *Farrell et al.* [1988] could explain the observed wave power if emitted electrons were modulated by strong beam-plasma interactions soon after leaving the FPEG aperture.

During TSS 1R events, beam electrons were emitted almost perpendicular to the magnetic field. In every case where ESA B intercepted beam fluxes $> \sim 8 \times 10^9$ (cm² s sr eV)⁻¹, modulations at megahertz frequencies were detected. Critical observations occurred when ESA B encountered beam electrons while looking toward the shuttle's left wing and ESA A faced FPEG. Early (late) in event 1 beam electrons were modulated near f_{ce} ($2f_{ce}$). During event 2 beam modulations were at $\sim 1.5 f_{ce}$. Modulations at the same frequencies were simultaneously observed in ESA A for 70 – 90 eV electrons. Both the beam and low-energy electrons had pitch angles of $\sim 90^\circ$. This appears to be consistent with the conjecture of *Farrell et al.* [1988] that beam electrons are modulated close to the FPEG emission site. Trajectories of the high and low energy modulated electrons reaching the ESAs intersect only in the immediate vicinity of FPEG. If the simultaneously detected modulations have the same cause, then it lies close to FPEG's aperture, perhaps as oscillations of a virtual cathode [*Hardy et al.*, 1995].

ESA A often detected modulations in the flux of electrons with sub-beam energies. The trajectories of all the modulated electrons were within the beam cylinder. In the proposed scenario these electrons would be influenced by the self-consistent electric fields generated by a modulating virtual cathode and the bunched beam electrons. This is reminiscent of wave-particle interactions known as electron cyclotron masers [*Lindsay*, 1981]. Ring distributions of energetic electrons in regions of varying ratios of the electron plasma and cyclotron frequencies are postulated to be sources of the auroral kilometric radiation observed in space [*Wu et al.*, 1982], and cyclotron radiation detected on the ground [*Wu et al.*, 1989]. Electron cyclotron maser waves are amplified by free energy in the energetic electron distribution. Here beam electrons appear to be

organized to drive intense cyclotron radiation directly at the large signal limit *Lindsay* [1981].

TSS 1 electron modulations at 2 – 4 MHz were attributed to upper-hybrid oscillations [*Gough et al.*, 1995]. TSS 1R modulations are related to cyclotron frequencies. On reexamination, the TSS 1 measurements appear to be consistent with those reported here. All but one of the modulation frequencies were $< f_{pe}$, and all were close to harmonics or odd half-harmonics of f_{ce} .

Acknowledgments. This work was supported by the Particle Physics and Astronomy Research Council of the UK, the U.S. Air Force Office of Scientific Research task 2311PL04, and Air Force contract F19628-96-K-0030 with Boston College.

References

- Farrell, W. M., D. A. Gurnett, P. M. Banks, R. I. Bush, and W. J. Raitt, An analysis of whistler mode radiation from the Spacelab 2 electron beam *J. Geophys. Res.*, **93**, 153-161, 1988.
- Gough, M. P., M. R. Oberhardt, D. A. Hardy, W. J. Burke, L. C. Gentile, B. McNeil, K. Bounar, D. C. Thompson, and W. J. Raitt, Correlator measurements of MHz wave-particle interactions during electron beam operations on STS-46, *J. Geophys. Res.*, **100**, 21561-21575, 1995.
- Goerke, R. T., P. J. Kellogg, and S. J. Monson, An analysis of whistler mode radiation from a 100 mA electron beam, *J. Geophys. Res.*, **95**, 4277-4283, 1990.
- Hardy, D. A., M. R. Oberhardt, W. J. Burke, D. C. Thompson, W. J. Raitt, and L. C. Gentile, Observations of electron beam propagation perpendicular to the earth's magnetic field during the TSS 1 Mission, *J. Geophys. Res.*, **100**, 21523-21534, 1995.
- Lindsay, P. A., Gyrotrons (electron cyclotron masers): Different mathematical models, *IEEE J. Quant. Electron.*, QE-17, 1327-1333, 1981.
- Maggs, J. E., Coherent generation of VLF, *J. Geophys. Res.*, **81**, 1707-1724, 1976.
- Wu, C. S., H. K. Wong, D. J. Gorney, and L. C. Lee, Generation of auroral kilometric radiation, *J. Geophys. Res.*, **87**, 4476-4487, 1982.
- Wu, C. S., P. H. Yoon, and H. P. Freund, A theory of electron cyclotron waves generated along auroral field lines observed by ground facilities, *Geophys. Res. Lett.*, **16**, 1461-1464, 1989.
- W. J. Burke, D. A. Hardy, and A. G. Rubin, Phillips Laboratory, 29 Randolph Road, Hanscom AFB, MA, 01731-3010. e-mail: burke@plh.af.mil; hardy@plh.af.mil; rubin@plh.af.mil
- A. T. Drobot, SAIC, 1710 Goodrich Dr., P.O. Box 1303, McLean, VA 22102. e-mail: drobot@mcclapo.saic.com
- L. C. Gentile and C. Y. Huang, Boston College Institute for Scientific Research, 402 St. Clement's Hall, 140 Commonwealth Avenue, Chestnut Hill, MA 02167-3862. e-mail: gentile@plh.af.mil, huang@plh.af.mil
- M. P. Gough, Space Science Centre, University of Sussex, Brighton, BN1 9QT, UK. email: m.p.gough@sussex.ac.uk
- M. R. Oberhardt, Amptek, Inc., 4 De Angelo Drive, Bedford, MA, 01730. email: moberhardt@amptek.com
- W. J. Raitt and D. C. Thompson, Center for Atmospheric and Space Sciences, Utah State University, Logan, UT, 84322-4405. email: raitt@cass.usu.edu; thompson@demise.cass.usu.edu

(Received January 13, 1997; revised September 25, 1997; accepted October 15, 1997.)